

Amplitude preserving AMO from true amplitude DMO and inverse DMO

Nizar Chemingui and Biondo Biondi¹

ABSTRACT

Starting from the definition of Azimuth Moveout (*AMO*) as the cascade of *DMO* and inverse *DMO* at different offsets and azimuths, we derive an amplitude-preserving function for the *AMO* operator. This amplitude function is based on the FK definition of *DMO* and the definition of its true inverse. Similar to Liner's formalism of a true inverse for Hale's *DMO*, we derive an asymptotically true inverse for Black/Zhang's *DMO* and Bleistein's Born *DMO*. A numerical test is given that compares amplitude preservation using kinematically equivalent *DMO* operators cascaded with their true inverses. We define amplitude-preserved processing as the preservation of the offset-dependent reflectivity after *AMO* transformation, where the reflectivity is considered to be proportional to the peak amplitude of each event. We found that an *AMO* operator defined using Zhang's *DMO* cascaded with its true inverse best reconstructs data amplitudes after transformation to a new offset and azimuth. The new amplitude function represents an amplitude-preserving azimuth moveout.

INTRODUCTION

Previously, Biondi and Chemingui (1994) introduced a partial-migration operator named Azimuth-Offset Moveout (*AMO*) that rotates the data azimuth and changes the data absolute offset. The *AMO* operator can be defined as the cascade of an imaging operator that acts on data with a given offset and azimuth, followed by a forward modeling operator that reconstructs the data at a different offset and azimuth.

In the context of amplitude preserving processing, we need to derive a true amplitude function for *AMO* so that amplitude variations as a function of offset and azimuth are not distorted by this operation. Because we derived *AMO* from *DMO*, *AMO* potentially has amplitude effects similar to those of *DMO*. Starting from the general definition of *DMO* in the FK domain (Zhang, 1988; ?) and the definition of a general inverse *DMO* (??), we derived inverses for Zhang's *DMO* and for Bleistein's Born *DMO*. Our derivation of true inverses is similar to that of Liner (?) for an amplitude-preserved inverse for Hale's *DMO*. The approach is based on a general formalism for inverting integral solutions (??) that we use to derive a solution for an integral inverse *DMO* that is asymptotically valid. Our motivation

¹email: nizar@sep.stanford.edu, biondo@sep.stanford.edu

for this approach is to compare our inverses to an inverse *DMO* formula of Ronen's (?) and Liner's (?). A best amplitude-preserving *DMO* cascaded with its true amplitude inverse is then selected to define an amplitude preserving *AMO*. We used this *AMO* operator in an amplitude-preserved processing sequence consisting of spherical divergence, normal-moveout (*NMO*), azimuth moveout (*AMO*) and inverse *NMO*.

We conducted numerical experiments by transforming data from a given azimuth and absolute offset to a new azimuth and offset using different *AMO* operators defined from kinematically equivalent *DMO*'s and inverse *DMO*'s. We tested for amplitude preservation by studying the offset-dependent reflectivity through peak amplitudes along a dipping event after the *AMO* transformation. According to most interpreters, "true-amplitude" means that each event's peak is proportional to the reflection coefficient.

In the next section we will briefly review the definition of the *AMO* operator, describe the general solution for an asymptotically valid inverse *DMO* (?) and then derive a true inverse for Zhang's *DMO* (1988) and Bleistein's Born *DMO* (?).

AZIMUTH MOVEOUT OPERATOR

We define *AMO* as an operator that transforms 3-D prestack data with a given offset and azimuth to equivalent data with different offsets and azimuths (Biondi and Chemingui, 1994). Figure ?? shows a graphical representation of this offset transformation; the input data with offset $\mathbf{h}_1 = h_1(\cos\theta_1, \sin\theta_1)$ is transformed into data with offset $\mathbf{h}_2 = h_2(\cos\theta_2, \sin\theta_2)$. *AMO* is not a single-trace to single-trace transformation, but moves events across midpoints according to their dip. Therefore, *AMO* is a partial-migration operator.

The *AMO* operator is defined in the the zero-offset frequency ω_o and midpoint wavenumber \mathbf{k} as

$$AMO = \int d\mathbf{k} e^{-i\mathbf{k}\cdot\mathbf{x}} \int dt_1 \int d\omega_o \mathbf{B} \mathbf{C} e^{i\omega_o \left(t_1 \sqrt{1 + \left(\frac{\mathbf{k}\cdot\mathbf{h}_1}{\omega_o t_1} \right)^2} - t_2 \sqrt{1 + \left(\frac{\mathbf{k}\cdot\mathbf{h}_2}{\omega_o t_2} \right)^2} \right)}. \quad (1)$$

The traveltimes t_1 and t_2 are, respectively, the traveltime of the input data after *NMO*, and the traveltime of the results before application of inverse *NMO*. \mathbf{B} and \mathbf{C} are the Jacobians in the FK definition of the *DMO* operator and the definition of its inverse DMO^{-1} .

Since 3-D prestack data are often irregularly sampled, it is necessary to define *AMO* as an integral operator in the time-space domain. A stationary-phase approximation of (1) yields a time-space representation of the *AMO* operator where the equation for the kinematics of the impulse response is (Biondi and Chemingui, 1994)

$$t_2(\mathbf{x}, \mathbf{h}_1, \mathbf{h}_2, t_1) = t_1 \frac{h_2}{h_1} \sqrt{\frac{h_1^2 \sin^2(\theta_1 - \theta_2) - x^2 \sin^2(\theta_2 - \varphi)}{h_2^2 \sin^2(\theta_1 - \theta_2) - x^2 \sin^2(\theta_1 - \varphi)}}, \quad (2)$$

while the amplitudes are given by

$$A(\mathbf{x}, \mathbf{h}_1, \mathbf{h}_2, t_1) \approx \frac{2\pi \mathbf{B} \mathbf{C}}{\sqrt{D}}, \quad (3)$$

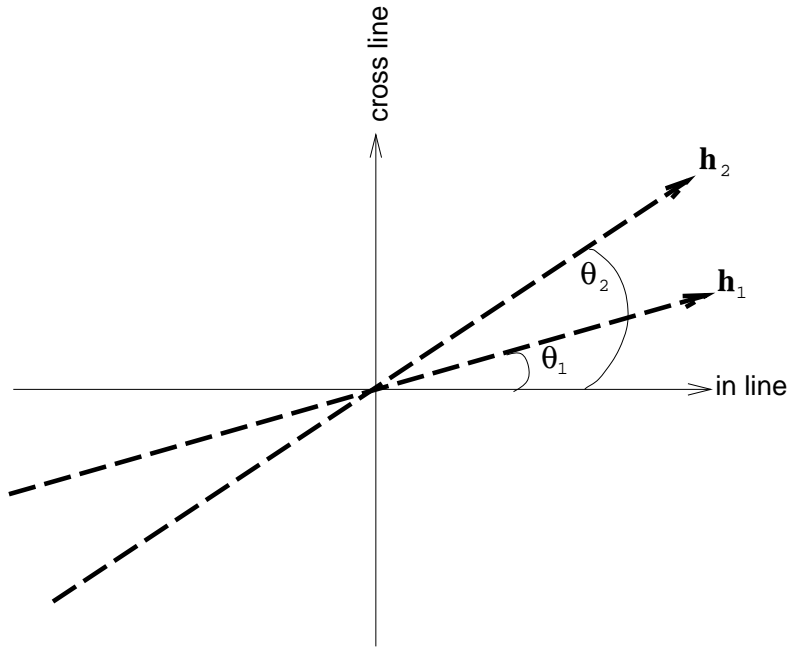


Figure 1: Map view of offset and azimuth of *AMO* input and output traces. nizar2-sketch
[NR]

where $\mathbf{x} = X(\cos \varphi, \sin \varphi)$ is the output location vector in midpoint coordinates and D is the determinant of a Hessian matrix. For given input half-offset and time (\mathbf{h}_1, t_1) and output half-offset (\mathbf{h}_2) , equations (2) and (3) define a surface in the time-midpoint space. The surface is a skewed saddle; its shape and spatial extent are controlled by the medium velocity, the absolute offsets and by the azimuth rotation, i.e., the differences in azimuths between the input and the output data (Biondi and Chemingui, 1994; Fomel and Biondi, 1995). The Jacobians \mathbf{B} and \mathbf{C} and the determinant Δ in equation (3) are actually evaluated at the stationary point of the phase function in the integral kernel of (1). We present an explicit formula for them for different cases of *DMO*'s in Appendix A.

The amplitude behavior of *AMO* is completely controlled by the amplitude functions of the *DMO* operator and its inverse. An amplitude correct *AMO* should follow from a true amplitude *DMO* and its amplitude-preserving inverse. Liner and Cohen (?) argued that an adjoint *DMO* operator is a poor representation of an inverse *DMO*. They showed that for the case of Hale *DMO*, the application of *DMO* followed by its adjoint inverse can result in a serious amplitude degradation. They proposed instead a solution for an asymptotically valid inverse *DMO* and derived a true inverse for Hale's *DMO*. In the next section we outline their solution and apply it in order

GENERAL FORMALISM FOR INVERSE DMO

DMO is a method of transformation of finite-offset data to zero-offset data. Let the normal moveout corrected input data be denoted $P_2(t_2, \mathbf{x}_2; \mathbf{h}_2)$ and the zero-offset desired output denoted $P_0(t_0, \mathbf{x}_0; \mathbf{h} = 0)$. Assume known relationships between the coordinates of the general form

$$t_0 = t_0(t_2, \mathbf{x}_2, w_0, \mathbf{k}_0) \quad \text{and} \quad \mathbf{x}_0 = \mathbf{x}_0(\mathbf{x}_2). \quad (4)$$

The *DMO* operator can be defined in the zero-offset frequency ω_0 and midpoint wavenumber \mathbf{k} as (?)

$$P_0(\omega_0, \mathbf{k}_0; \mathbf{h} = 0) = \int d\mathbf{x}_2 \frac{d\mathbf{x}_0}{d\mathbf{x}_2} \int dt_2 \frac{dt_0}{dt_2} e^{[i\omega_0 t_0(t_2) - \mathbf{k}_0 \cdot \mathbf{x}_0(\mathbf{x}_2)]} P_2(t_2, \mathbf{x}_2; \mathbf{h}_2) \quad (5)$$

$$= \int d\mathbf{x}_2 \int dt_2 \mathbf{B} e^{[i\omega_0 t_0(t_2) - \mathbf{k}_0 \cdot \mathbf{x}_0(\mathbf{x}_2)]} P_2(t_2, \mathbf{x}_2; \mathbf{h}_2), \quad (6)$$

whereas its inverse can be defined as:

$$P_2(t_2, \mathbf{x}_2; \mathbf{h}_2) = \int d\mathbf{k}_0 \int d\omega_0 \mathbf{C} e^{-[i\omega_0 t_0(t_2) - \mathbf{k}_0 \cdot \mathbf{x}_0(\mathbf{x}_2)]} P_0(\omega_0, \mathbf{k}_0; \mathbf{h} = 0) \quad (7)$$

where

$$\mathbf{C} = \mathbf{C}(t_2, \mathbf{x}_2, \omega_0, \mathbf{k}_0) \quad (8)$$

Note that for consistency with our definition of the *AMO* operator we consider a DMO^{-1} for a forward *DMO* that reconstructs a zero-offset section $P_0(t_0, \mathbf{x}_0; \mathbf{h} = 0)$ from an input section $P_2(t_2, \mathbf{x}_2; \mathbf{h}_2)$ recorded at a finite vector-offset \mathbf{h}_2 .

A detailed derivation of \mathbf{C} is given by Liner (?). The method is based on a general formalism (??) for inverting integral equations such as (6). The technique mainly involves inserting (6) into (7) and expanding the resulting amplitude and phase as a Taylor series and making a change of variables according to Beylkin (?). The solution provides an asymptotic inverse for (6), where the weights are given by

$$\mathbf{C} = \frac{d\omega}{d\omega_0} \frac{d\mathbf{k}}{d\mathbf{k}_0} \left[4\pi^2 \frac{dt_0}{dt_2} \frac{d\mathbf{x}_0}{d\mathbf{x}_2} \right]^{-1} \quad (9)$$

In this expression, $\mathbf{B} = \frac{dt_0}{dt_2} \frac{d\mathbf{x}_0}{d\mathbf{x}_2}$ is the Jacobian of the change of variables in the forward *DMO* given by

$$\mathbf{B} = \frac{\partial(t_0, \mathbf{x}_0)}{\partial(t_2, \mathbf{x}_2)} = \det \begin{bmatrix} \frac{dt_0}{dt_2} & \frac{d\mathbf{x}_0}{d\mathbf{x}_2} \\ \frac{d\mathbf{x}_0}{dt_2} & \frac{d\mathbf{x}_0}{d\mathbf{x}_2} \end{bmatrix} \quad (10)$$

which reduces to $J = \frac{dt_0}{dt_2} \frac{d\mathbf{x}_0}{d\mathbf{x}_2}$ assuming the general coordinate relationships (4) where \mathbf{x}_0 is independent of t_2 , leading to a zero lower left element in the determinant matrix above.

The quantity $\frac{d\omega}{d\omega_0} \frac{d\mathbf{k}}{d\mathbf{k}_0}$ is the inverse of the Beylkin determinant, H ,

$$H = \frac{\partial(\omega_0, \mathbf{k}_0)}{\partial(\omega, \mathbf{k})} = \det \begin{bmatrix} \frac{d\omega_0}{d\omega} & \frac{d\omega_0}{d\mathbf{k}} \\ \frac{d\mathbf{k}_0}{d\omega} & \frac{d\mathbf{k}_0}{d\mathbf{k}} \end{bmatrix}. \quad (11)$$

We actually compute the inverse of H as given by Liner (?):

$$H^{-1} = \frac{\partial(\omega, \mathbf{k})}{\partial(\omega_0, \mathbf{k}_0)} = \det \begin{bmatrix} \frac{d\omega}{d\omega_0} & \frac{d\omega}{d\mathbf{k}_0} \\ \frac{d\mathbf{k}}{d\omega_0} & \frac{d\mathbf{k}}{d\mathbf{k}_0} \end{bmatrix}. \quad (12)$$

If we recognize that \mathbf{k} is independent of ω_0 , then the lower element of H^{-1} is zero and (12) reduces to

$$H^{-1} = \frac{d\omega}{d\omega_0} \frac{d\mathbf{k}}{d\mathbf{k}_0}, \quad (13)$$

where ω and \mathbf{k} are, respectively,

$$\omega = \omega_0 \frac{d}{dt_2} [t_0(t_2)] \quad (14)$$

$$\mathbf{k} = \mathbf{k}_0 \frac{d}{d\mathbf{x}_2} [\mathbf{x}_0(\mathbf{x}_2)]. \quad (15)$$

It is very important to recognize at this stage that ω and \mathbf{k} in equations (14) and (15) depend on the coordinate relationships (4). Therefore, the Beylkin determinant, H , is different for different *DMO* operators. However, as we will demonstrate later, for kinematically equivalent *DMO* operators the determinant is constant. We conclude that a general inverse *DMO* is completely defined given the coordinate relationships connecting output time and mid point to their input values. The asymptotic inverse represents an amplitude-preserving inverse *DMO*. The methodology was first applied to Hale's *DMO* by Liner and Cohen (?), and we outline their results in the next section.

Hale DMO and its inverse

Starting from the coordinate relationships between a finite-offset data and its equivalent zero-offset data

$$t_0 = t_2 \left[1 + \left(\frac{\mathbf{k} \cdot \mathbf{h}_2}{\omega_0 t_2} \right)^2 \right]^{1/2} \equiv t_2 A_2 \quad \text{and} \quad \mathbf{x}_0 = \mathbf{x}_2 \quad (16)$$

After differentiating (16) and taking into account a factor of $1/2\pi$ as scaling for the spatial Fourier transform we can write (9) as

$$\mathbf{C} = \frac{A_2}{2\pi} \frac{d\omega}{d\omega_0} \frac{d\mathbf{k}}{d\mathbf{k}_0}. \quad (17)$$

The remaining task reduces to performing the necessary derivatives, and with some algebra one can verify that H reduces to the simple expression (?)

$$H = \frac{A_2^3}{2A_2^2 - 1} \quad (18)$$

and, therefore, we arrive at the inversion amplitude function

$$\mathbf{C} = \frac{1}{2\pi} \left[1 + \frac{\mathbf{k}^2 \mathbf{h}^2}{\omega_o^2 t_2^2 A_2^2} \right]. \quad (19)$$

For a detailed derivation, the reader should refer to the original work of Liner (?). An asymptotic true inverse for Hale's *DMO* should then have the form:

$$P_2(t_2, \mathbf{x}_2; \mathbf{h}_2) = \frac{1}{2\pi} \int d\mathbf{k}_0 \int d\omega_o \left[1 + \frac{\mathbf{k}^2 \mathbf{h}^2}{\omega_o^2 t_2^2 A_2^2} \right] e^{-[i\omega_o A_2 t_2 - \mathbf{k}_0 \cdot \mathbf{x}_0(\mathbf{x}_2)]} P_0(\omega_o, \mathbf{k}_0; \mathbf{h} = 0) \quad (20)$$

Black/Zhang *DMO* and its inverse

Similar to the preceding discussion, we start our derivation for an asymptotic inverse for Black/Zhang's *DMO* by recognizing the coordinate relationships,

$$t_0 = t_2 A_2^{-1} \quad \text{and} \quad \mathbf{x}_0 = \mathbf{x}_2 - \frac{\mathbf{k} \mathbf{h}^2}{\omega_o t_2 A_2} \quad (21)$$

The Jacobian of the change of variables in the forward *DMO* is given by

$$\mathbf{B} = \frac{\partial(t_0, \mathbf{x}_0)}{\partial(t_2, \mathbf{x}_2)} = \frac{2A_2^2 - 1}{A_2^3}, \quad (22)$$

which has the familiar form of Zhang's (1988) and Black's (1993) Jacobian. Zhang based his derivations on kinematic arguments that considered a fixed reflection point rather than a fixed midpoint. This derivation takes into account the reflection-point smear (Deregowski and Rocca, 1981; ?), which means that the input event at location \mathbf{x}_2 will be positioned by *DMO* to the correct zero-offset location \mathbf{x}_0 .

To compute the Beylkin determinant for Black/Zhang Jacobian we start by writing the phase phase function in the *DMO* integral kernel as:

$$\Phi = \omega t_0 - \mathbf{k} \cdot \mathbf{x}_0 \quad (23)$$

$$= \omega \frac{t_2}{A_2} - \mathbf{k} \cdot \left(\mathbf{x}_2 - \frac{\mathbf{k} \mathbf{h}^2}{\omega_o t_2 A_2} \right) \quad (24)$$

$$= \omega \frac{t_2}{A_2} - \mathbf{k} \cdot \mathbf{x}_2 + \omega_o t_2 \left(\frac{A_2^2 - 1}{A_2} \right) \quad (25)$$

$$= \omega A_2 t_2 - \mathbf{k} \cdot \mathbf{x}_2 \quad (26)$$

The phase in equation (26) is identical to the phase function in Hale's *DMO* and, therefore, substituting for ω and \mathbf{k} back in (14) and (15) and differentiating with respect to ω_0 and \mathbf{k}_0 , we end up with the following expression for H^{-1} :

$$H^{-1} = \frac{A_2^3}{2A_2^2 - 1}. \quad (27)$$

Therefore, the Beylkin determinant for Black/Zhang's *DMO* becomes

$$H = \frac{2A_2^2 - 1}{A_2^3} \quad (28)$$

which is the same as that for Hales's *DMO*.

Finally, by substituting back in (9) and accounting for the $1/2\pi$ factor in the spatial Fourier transform, we obtain an expression for the weights of an asymptotic inverse for Black/Zhang's *DMO*:

$$\mathbf{C} = \frac{1}{2\pi} \quad (29)$$

These weights have been also derived independently by Paul Fowler (personal communication). Therefore, a true inverse for Black/Zhang's (1988) *DMO* has the form

$$P_2(t_2, \mathbf{x}_2; \mathbf{h}_2) = \frac{1}{2\pi} \int d\mathbf{k}_0 \int d\omega_o e^{-[i\omega_o A_2 t_2 - \mathbf{k}_0 \cdot \mathbf{x}_0(\mathbf{x}_2)]} P_0(\omega_0, \mathbf{k}_0; \mathbf{h} = 0) \quad (30)$$

Bleistein Born *DMO* and its inverse

Starting from a different argument, Bleistein (?) proposed a *DMO* operator that he derived from a Born approximation for modeling wave propagation. This new operator, named Born *DMO* (*BDMO*), is kinematically equivalent to Hale's (1984) *DMO* and Zhang's (1988) *DMO* and only differs from each of them by a simple amplitude factor. This new Jacobian is defined as

$$\mathbf{B} = \frac{\partial(t_0, \mathbf{x}_0)}{\partial(t_2, \mathbf{x}_2)} = \frac{2A_2^2 - 1}{A_2}. \quad (31)$$

Similar to the previous analysis, and recognizing that this *BDMO* is kinematically equivalent to Hale's *DMO*, we derive the weights on the inverse for Bleistein's operator as

$$\mathbf{C} = \frac{1}{2\pi A_2^2}. \quad (32)$$

An asymptotic true inverse for Born *DMO* is, then,

$$P_2(t_2, \mathbf{x}_2; \mathbf{h}_2) = \frac{1}{2\pi} \int d\mathbf{k}_0 \int d\omega_o \frac{1}{A_2^2} e^{-[i\omega_o A_2 t_2 - \mathbf{k}_0 \cdot \mathbf{x}_0(\mathbf{x}_2)]} P_0(\omega_0, \mathbf{k}_0; \mathbf{h} = 0) \quad (33)$$

Summary of true inverse for FK DMO

In this section we analyze the concept of an asymptotic true inverse and relate it to our application of *AMO*. Figures ?? and 3 compare results of different inverse *DMO* operators. Figure ?? is similar to the spike test of Liner (?). The left plot is an in-line section from a common offset cube consisting of five unit-amplitude spikes. The offset is 800m and the CMP spacing is 20 m in both directions. We compare the output of each true inverse to the output of Ronen (?) inverse. The ideal output would be five spikes with unit amplitudes. The table below summarizes the output of each inverse *DMO* for increasingly deep spikes.

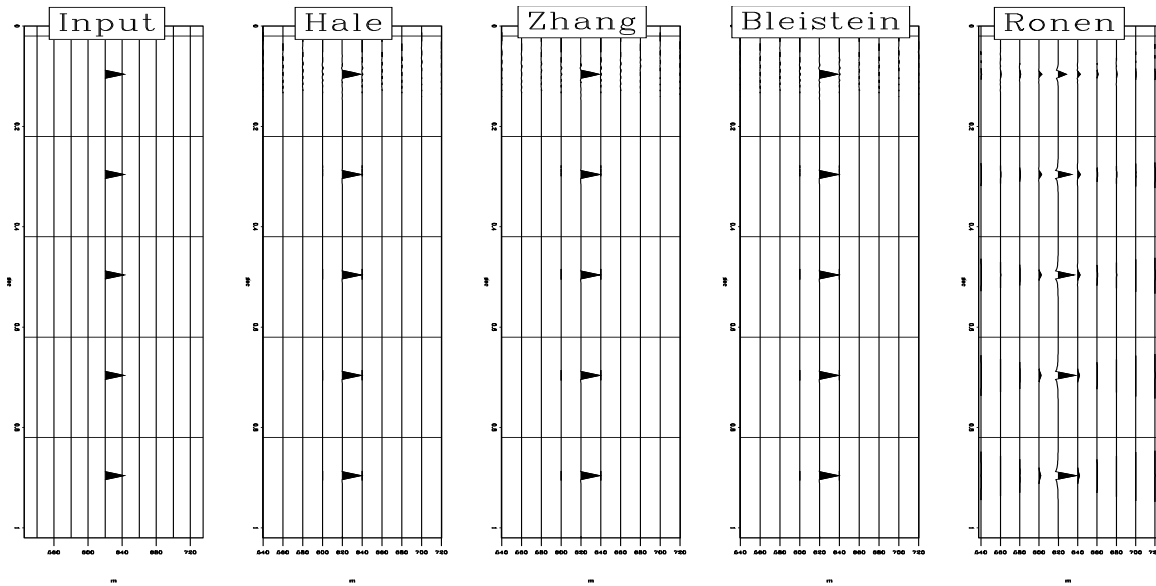


Figure 2: From left to right: input data, results from Hale's inverse, Black/Zhang's inverse, Bleistein's inverse and Ronen's inverse. [nizar2-Spike](#) [ER]

IDEAL Amp.	Hale	Black/Zhang	Bleistein	Ronen
1.00	.76	.76	.76	.35
1.00	.95	.95	.95	.66
1.00	.97	.97	.97	.77
1.00	.97	.97	.97	.82
1.00	.98	.98	.98	.86

Figure 3 consists of a similar test on an input earth model consisting of a single bed dipping 35 degrees. The original input section is a constant-offset section recorded at half offset of 800 m with 25 m CMP spacing. The input to each DMO^{-1} is the output of its corresponding forward *DMO* operator. We plot the peak amplitudes picked along the dipping event from the output of each inverse *DMO*. The curves of amplitude picks from all three inverses perfectly coincide with the amplitude picks from the original input section (*DMO* input). On the same graph we also plot the peak amplitudes extracted from the output of Ronen's inverse. The results of this inverse clearly fall below their expected values.

For both tests the results from the three different *DMO*'s analyzed were identical. This behavior follows directly from the kinematic equivalence of each of these *DMO* operators. On the spike test we also notice that the results of the inversion are more accurate from the shallowest to the deepest spike illustrating the asymptotic nature of the true inverse. Note that the two tests are only conclusive on the accuracy of the inverse *DMO* solution. Since we are interested in the cascade of both forward and inverse operators acting at two different offsets and azimuths, we need to understand what happens in the intermediate mapping to zero offset prior to the forward modeling step.

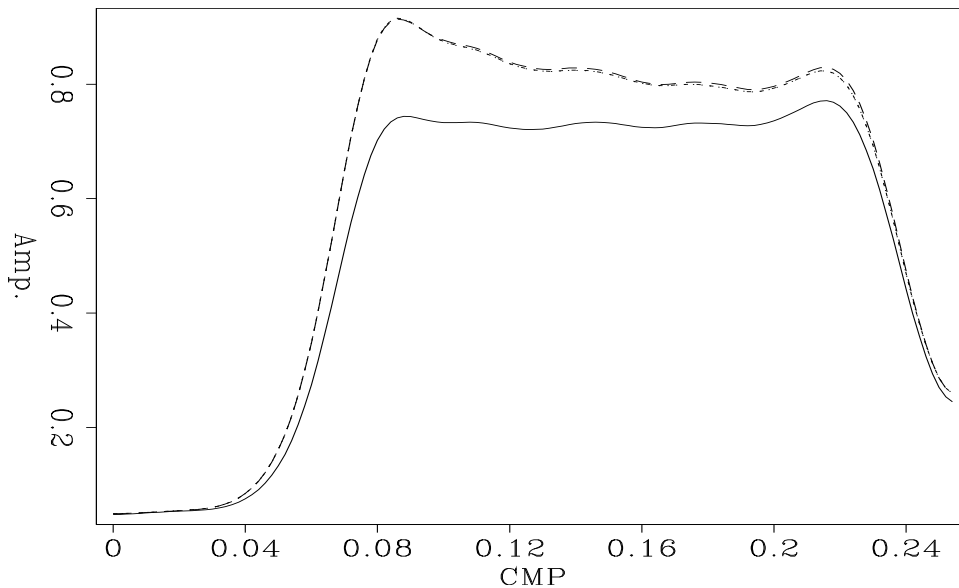


Figure 3: Peak amplitudes along the dipping event from the output of various inverse *DMO* algorithms. The lower amplitude curve is the result of applying Ronen's inverse. The results from Hale, Zhang, and Bleistein inverses are exactly the same and coincide with the predicted peak amplitudes from the synthetic input. `nizar2-comp-idmo` [ER]

TRUE AMPLITUDE AMO FROM TRUE AMPLITUDE DMO

Our goal is to define an amplitude-preserving *AMO* from a true amplitude *DMO* and its true amplitude inverse. The definition of a true amplitude inverse follows directly from an amplitude-preserving forward operator. To select a true amplitude *DMO* we compare the behavior of various *DMO* algorithms on a dipping bed. Figure 4 shows the peak amplitudes picked along the reflection event from the output of several forward *DMO* operators. The input data is a constant offset section modeled with a 3-D Kirchhoff style modeling algorithm. The input was corrected for spherical-divergence spreading and for *NMO* effects. On the same plot we also superimpose the peak amplitudes from a zero-offset section generated with the Kirchhoff modeling program. As we notice, the theoretical curve almost coincides with the output amplitudes of Zhang *DMO*. The amplitudes given by Hale's algorithm fall below the theoretical curve whereas the peak-amplitude from Bleistein's output overshoot the correct

amplitudes. To understand this behavior we need to examine the difference between what each *DMO* is trying to accomplish.

The difference between Bleistein’s *DMO* and Black/Zhang’s *DMO* results from a philosophical difference about what could be defined as “true-amplitude *DMO*”. While our goal was preserving the peak amplitude of each reflection event, Bleistein’s algorithm is based on preserving the spectral density of the image wavelet. A second difference results from the sequence in the processing flow surrounding *DMO*. A divergence correction must be applied to the input prior to applying Black/Zhang’s *DMO*, whereas both input and output of Bleistein’s *DMO* decay with spherical divergence factors of $\frac{1}{t_2}$ and $\frac{1}{t_0}$ respectively (?). These two differences account for the A^2 factor between the two Jacobians leading to higher weights on Bleistein’s *DMO*, which results in higher peak amplitude than those on the predicted curve.

On the other hand, the difference between Black/Zhang’s *DMO* and Hale’s *DMO* results from the fact that the former algorithm accounts for the reflection point smear and, therefore, correctly repositions input events at their true zero-offset locations. The two Jacobians differ by a factor of

$$\frac{B_Z}{B_H} = \frac{2A^2 - 1}{A^2} \quad (34)$$

Because this ratio being always larger than 1, it leads to lower weights on Hale’s operator, which explains the lower peak amplitudes measured along the dipping event in the output of Hale’s *DMO*.

Consequently, to be consistent with our original definition of “amplitude preserved processing”, we chose to define the amplitude function for the *AMO* operator from the Jacobian of Black/Zhang’s *DMO* and the Jacobian of its corresponding asymptotic true inverse. In the remainder of the paper we examine the amplitude behavior of *AMO* according to this definition.

AMPLITUDE PRESERVATION BY AMO

The *AMO* operator is defined as the cascade of an imaging operator that acts on data with a given offset and azimuth, followed by a forward modeling operator that reconstructs the data at a different offset and azimuth. *AMO* can also be defined as the cascade of an offset continuation operator that changes the data absolute offset followed by an azimuth continuation operator that rotates the data azimuth. These two operations do commute and in some applications the *AMO* operation may reduce to simply one or the other.

To examine the amplitude behavior of *AMO*, we conducted various numerical experiments and tested for amplitude preservation for a dipping reflector. In a first experiment we apply *AMO* as an azimuth continuation operator to change the orientation of the input. In a second test *AMO* acts a 2-D offset continuation that modifies the offset of the data. In a final test we apply *AMO* as a vector-offset continuation operator where both offset and azimuth are modified during the transformation. For each experiment we compare the peak amplitudes

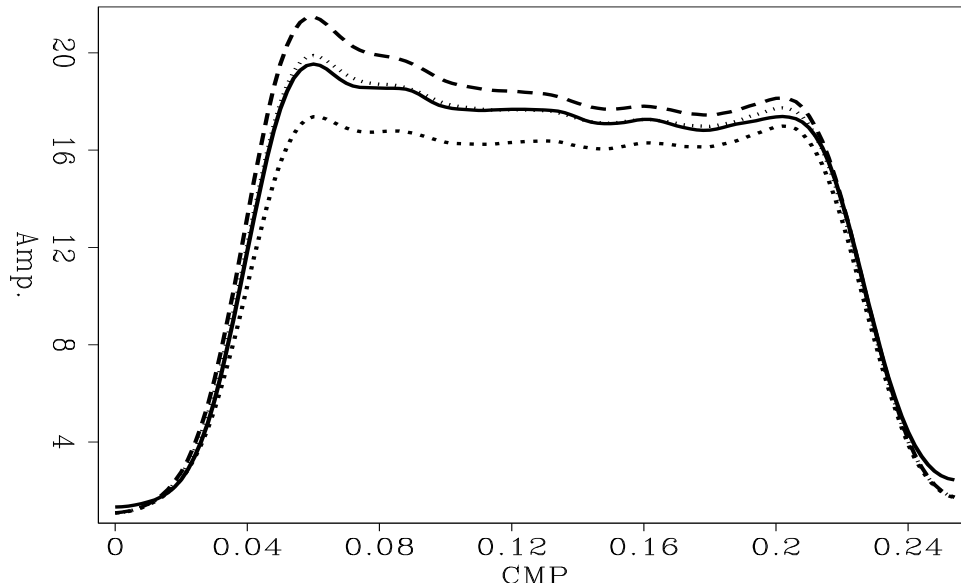


Figure 4: Peak amplitudes along the dipping event from the output of various DMO algorithms. The continuous curve is the the predicted result, the dashed curve is Hale's result, the dotted curve is Black/Zhang's results and the large dashed curve (top curve) is Bleistein's result `nizar2-comp-dmo` [NR]

picked on the *AMO* reconstructed sections to the peak amplitudes extracted from identical sections generated by synthetic modeling. To better illustrate the difference in amplitudes, we slightly smooth the curves of amplitude picks on both sections

Azimuth continuation

Starting from an an input constant-offset section recorded at half offset of 800 m and an angle of 5 degrees measured from the dip direction, we rotate the azimuth of the data by 40 degrees while keeping the offset constant. We compare the reconstructed section to a constant offset section modeled by the 3-D modeling code at an offset of 800m and azimuth of 45 degrees. Figure 5 shows the peak amplitudes extracted from the output of *AMO* along the dipping event. On the same graph we also plot the peak amplitudes as picked from the modeled section. Note that the two curves are very similar with the reconstructed amplitudes being few percent lower than the predicted peak amplitudes.

Offset continuation

In the case of no azimuthal change, *AMO* reduces to a 2-dimensional operator that is equivalent to an offset continuation operator. We apply *AMO* to the same input constant-offset section recorded at half offset 800m and 5-dgree azimuth to change its offset to 400m. Figure 6 shows the peak amplitudes picked along the dipping event on the reconstructed section to-

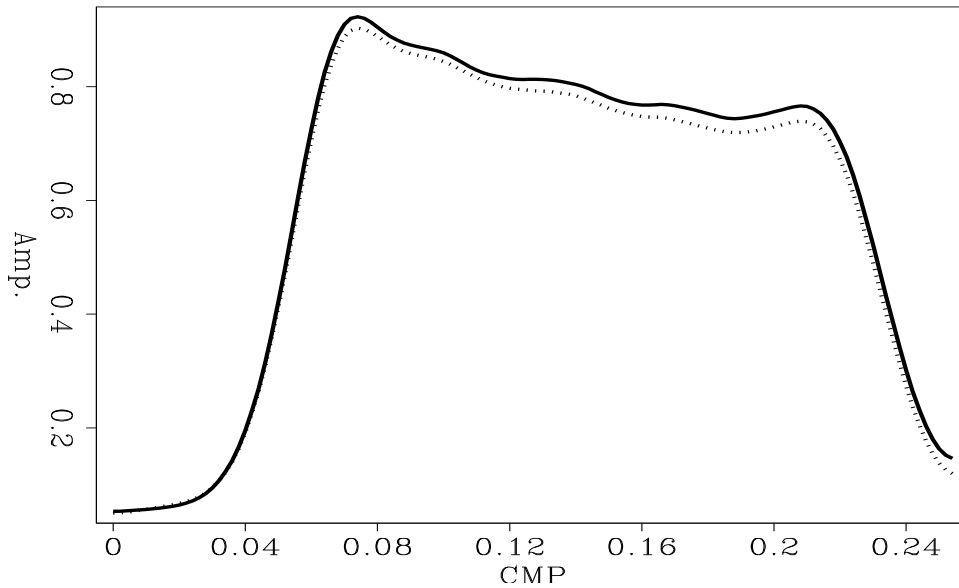


Figure 5: Peak amplitudes extracted from azimuth continued section (dashed curve) and from synthetic section (continuous plot). `nizar2-azimuth` [ER]

gether with the theoretical curve from the modeling program. Again we notice that both plots follow each other very closely with an error of less than a few percent.

Vector-offset continuation

In a final experiment we apply the *AMO* operator to transform the input constant-offset section of the first test to a new section with different absolute half offset of 400m and azimuth of 45 degrees. Figure 7 shows the peak amplitudes picked along the dipping event on the reconstructed section. For comparison, we also plot the peak amplitudes from a reference section that is modeled with the same vector offset as the output of *AMO*. The two curves match very closely and the differences are more contributed to cumulative errors in the processing sequence surrounding *AMO*, which includes spherical divergence and *NMO* corrections prior to *AMO* and inverse *NMO* after *AMO*.

CONCLUSION

We presented an amplitude-preserving function for the *AMO* operator. This amplitude function is based on the FK definition of *DMO* and the definition of its true inverse. Similar to Liner's formalism of a true inverse for Hale's *DMO*, we derived an asymptotically true inverse for Black/Zhang's *DMO* and Bleistein's Born *DMO*. Numerical experiments showed that Black/Zhang *DMO* best preserves peak amplitudes. We define amplitude-preserved processing as the preservation of the offset-dependent reflectivity after *AMO* transformation, where the reflectivity is considered to be proportional to the peak amplitude of each event. We used

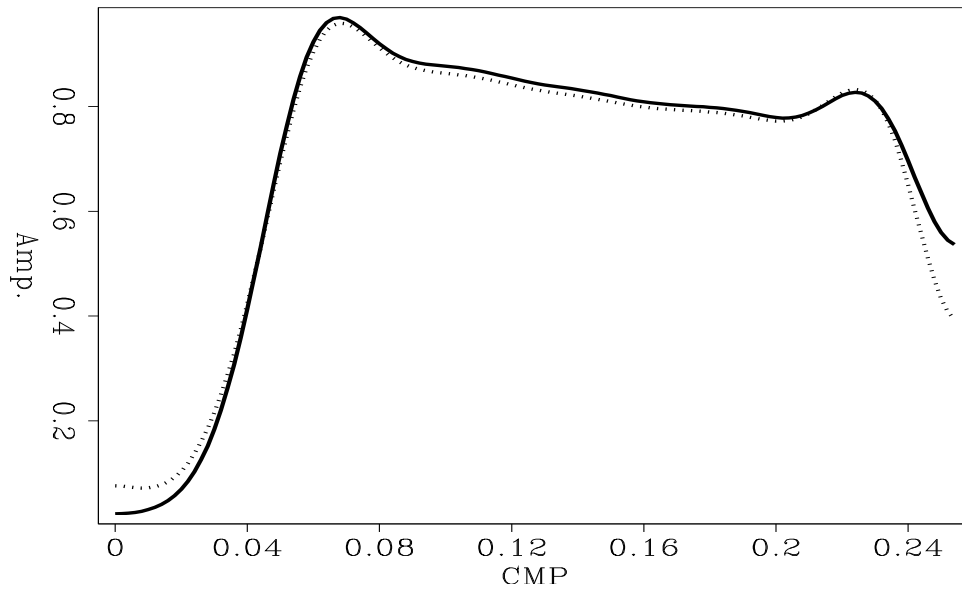


Figure 6: Peak amplitudes from offset-continued section from $h_1=800\text{m}$ to $h_2=400\text{m}$ and from a synthetic curve modeled at $h=400\text{m}$ (continuous curve). `nizar2-offset` [ER]

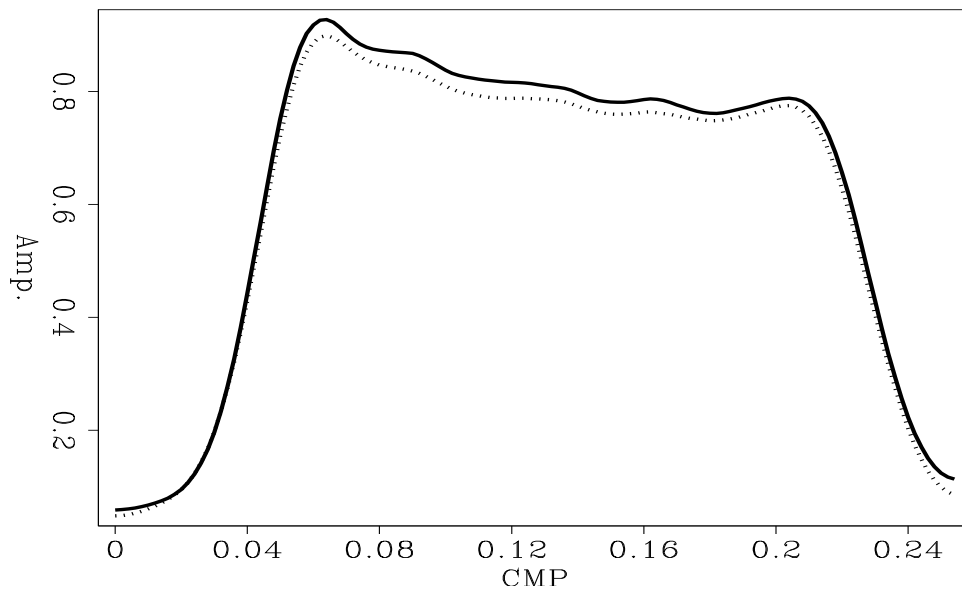


Figure 7: Peak amplitudes extracted from a section rotated by 40 degrees and offset continued from 800m to 400m. The solid curves shows the predicted amplitudes from the synthetic section. `nizar2-amo` [ER]

Black/Zhang's *DMO* cascaded with its true inverse to define an amplitude function for the AMO operator. Results showed that we can preserve peak amplitudes for a dipping event after applying AMO as an azimuth continuation operator, as an offset continuation operator or a vector-offset transformation. We conclude that the new AMO amplitude function represents an amplitude-preserving azimuth moveout.

ACKNOWLEDGMENTS

We thank Norman Bleistein, Paul Fowler, Chris Liner and Mihai Popovici for useful discussions on DMO. David lumley helped define the problem of true amplitude processing.

APPENDIX A

CONNECTING FK AMO WITH INTEGRAL AMO

This appendix describes the derivation of the amplitude function for the AMO impulse response in the time-space domain. The determinant D in Equation (3) of the main text can be written in terms of Biondi and Chemingui (1994) notations as:

$$\begin{aligned}
 D &= -\frac{(h_{2x}h_{1y} - h_{1x}h_{2y})^2}{\omega_o^2 t_1 t_2} (1 + \beta_1^2)^{-3/2} (1 + \beta_2^2)^{-3/2} \\
 &= -\frac{\Delta^2}{\omega_o^2 t_1 t_2} (1 + \beta_1^2)^{-3/2} (1 + \beta_2^2)^{-3/2} \\
 &= -\frac{\Delta^2}{\omega_o^2 t_1^2} A_1^{-4} A_2^{-2}.
 \end{aligned} \tag{A-1}$$

where β_1 and β_2 are, respectively,

$$\beta_1 = \frac{\mathbf{h}_1 \cdot \mathbf{k}}{\omega_o t_1} \quad \text{and} \quad \beta_2 = \frac{\mathbf{h}_2 \cdot \mathbf{k}}{\omega_o t_2} \tag{A-2}$$

and Δ is given by:

$$\begin{aligned}
 \Delta &= h_{2x}h_{1y} - h_{1x}h_{2y} \\
 &= |h_1||h_2|\sin(\theta_1 - \theta_2)
 \end{aligned} \tag{A-3}$$

Using a similar change of variable as used for the solution to the stationary path (Biondi and Chemingui, 1994), we write

$$v_1 = \frac{\beta_1}{\sqrt{1 + \beta_1^2}} \quad \text{and} \quad v_2 = \frac{\beta_2}{\sqrt{1 + \beta_2^2}}. \tag{A-4}$$

where v_1 and v_2 , evaluated at the stationary path \mathbf{k}_0 are

$$v_1 = \frac{X \sin(\theta_2 - \varphi)}{h_1 \sin(\theta_1 - \theta_2)}, \quad (\text{A-5})$$

and

$$v_2 = \frac{X \sin(\theta_1 - \varphi)}{h_2 \sin(\theta_1 - \theta_2)}. \quad (\text{A-6})$$

Next we substitute for (A-4) and (A-5) in (A-2) to evaluate the determinant D at the stationary path. In a final step we evaluate the forward and inverse Jacobians at the stationary path and substitute back for \mathbf{B} , \mathbf{C} and D in equation (3) of the main text. We obtain the following expressions for the amplitude function of the *AMO* operator as defined in terms of various *DMO* operators and their corresponding inverses.

Hale weights

$$A(\mathbf{x}, \mathbf{h}_1, \mathbf{h}_2, t_1) = \frac{\omega_o t_1}{\Delta} \left(\frac{(1 + v_2^2)}{\sqrt{1 - v_1^2} \sqrt{1 - v_2^2}} \right) \quad (\text{A-7})$$

Black/Zhang weights

$$A(\mathbf{x}, \mathbf{h}_1, \mathbf{h}_2, t_1) = \frac{\omega_o t_1}{\Delta} \left(\frac{(1 + v_2^2)}{(1 - v_1^2)^{3/2} (1 - v_2^2)^{1/2}} \right) \quad (\text{A-8})$$

Bleistein weights

$$A(\mathbf{x}, \mathbf{h}_1, \mathbf{h}_2, t_1) = \frac{\omega_o t_1}{\Delta} \left(\frac{(1 + v_2^2)(1 - v_2^2)^{1/2}}{(1 - v_1^2)^{3/2}} \right) \quad (\text{A-9})$$

Notice that the zero-offset frequency ω_o enters as multiplicative factor in the expression for *AMO* amplitudes, but the data is never available as zero-offset data during the *AMO* process. The effect of this multiplicative factor can be approximated by a time-domain filter applied either to the input or to the output data (Biondi and Chemingui, 1994).

REFERENCES

Biondi, B., and Chemingui, N., 1994, Transformation of 3-D prestack data by Azimuth Move-out: 64th Ann. Internat. Meeting, Soc. Expl. Geophys., Expanded Abstracts, 1541–1544.

Deregowski, S. M., and Rocca, F., 1981, Geometrical optics and wave theory of constant offset sections in layered media: *Geophys. Prosp.*, **29**, no. 3, 374–406.

Fomel, S., and Biondi, B., 1995, The time and space formulation of azimuth moveout: *SEP-84*, ??–??.

Hale, D., and Artley, C., 1993, Squeezing dip moveout for depth-variable velocity: *Geophysics*, **58**, 257–264.

Zhang, L., 1988, A new Jacobian for dip moveout: *SEP-59*, 201–208.

